Biophysical Journal Volume 73 November 1997 2376–2392

# Molecular Dynamics of Individual α-Helices of Bacteriorhodopsin in Dimyristoyl Phosphatidylcholine. I. Structure and Dynamics

Thomas B. Woolf

Departments of Physiology and of Biophysics and Biophysical Chemistry, Johns Hopkins University, School of Medicine, Baltimore, Maryland 21205 USA

ABSTRACT Understanding the role of the lipid bilayer in membrane protein structure and dynamics is needed for tertiary structure determination methods. However, the molecular details are not well understood. Molecular dynamics computer calculations can provide insight into these molecular details of protein:lipid interactions. This paper reports on 10 simulations of individual α-helices in explicit lipid bilayers. The 10 helices were selected from the bacteriorhodopsin structure as representative α-helical membrane folding components. The bilayer is constructed of dimyristoyl phosphatidylcholine molecules. The only major difference between simulations is the primary sequence of the α-helix. The results show dramatic differences in motional behavior between α-helices. For example, helix A has much smaller root-mean-squared deviations than does helix D. This can be understood in terms of the presence of aromatic residues at the interface for helix A that are not present in helix D. Additional motions are possible for the helices that contain proline side chains relative to other amino acids. The results thus provide insight into the types of motion and the average structures possible for helices within the bilayer setting and demonstrate the strength of molecular simulations in providing molecular details that are not directly visualized in experiments.

## INTRODUCTION

Understanding the restrictions imposed by the lipid bilayer environment on membrane protein structure and dynamics is needed for the successful prediction of membrane protein tertiary structure. This coupling between environment and protein is relatively well understood for globular proteins and very poorly characterized for membrane proteins. This is partly due to the homogeneous environment for globular proteins and the heterogeneous environment for membrane proteins. It is also a reflection of the relative lack of tertiary structural information for membrane proteins relative to the situation for globular proteins. This has made detailed molecular modeling of the interaction of membrane proteins with their environment difficult.

Molecular level simulations of lipid bilayers and of bilayers with membrane proteins have been dependent on new methods for the generation of initial states and on potential functions that are parametrized for protein:lipid interactions. Only recently have methods converged to the point where simulations of bilayer dynamics are possible (e.g., see Merz and Roux, 1996). The initial state difficulties can be understood as the long relaxation times needed for large amphipathic lipid molecules on the molecular dynamics time scale. Solvation in a water medium is much easier than in membrane systems because the relaxation time for the water molecules is relatively fast (e.g., see Brooks et al., 1988). With proper attention to the details of the initial simulation set-up and with well determined potential functions (Schlenkrich et al., 1996), it is now clear that meaningful results can be calculated (e.g., see Bassolino-Klimas et al., 1993; Venable et al., 1993; Pastor, 1994; Damodaran et al., 1995; Woolf and Roux, 1994, 1996). The resulting methods are computer-intensive, but provide considerable microscopic insight into details of motion and interaction that are not directly available to experiment or less detailed computer models. This has set the stage for the possibility of constructing representations of known membrane proteins within the explicit bilayer setting, but the large size of known membrane protein structures has made it difficult to immediately perform a direct simulation of a full protein system and lipid. For example, a simulation of the photosynthetic reaction center or of the recent cytochrome c oxidase structures with explicit lipid would be a system with on the order of 20,000 or more atoms. At present, a detailed consideration of simplified model systems can give molecular insight into motions and interactions that will be present in larger, more complex systems as well as providing details important for a discussion of protein folding.

The recent development of an algorithm for the construction of initial starting points for protein:lipid systems used gramicidin in dimyristoyl phosphatidylcholine (DMPC) (Woolf and Roux, 1994, 1996). An advantage of the gramicidin system relative to the current system is the availability of solid-state NMR data for direct comparison with the simulations. The construction method uses a library of preequilibrated and prehydrated DMPC lipid molecules that represent the liquid crystalline state of the bilayer. This allows a much more rapid approach to a realistic starting point than is possible with gel-state starting conditions. The

*Received for publication 13 January 1997 and in final form 13 August 1997.*

Address reprint requests to Dr. Thomas Woolf, Departments of Physiology and of Biophysics and Biophysical Chemistry, Johns Hopkins University, School of Medicine, 725 N. Wolfe St., Baltimore, MD 21205. Tel.: 410-614-2643; Fax: 410-955-0461; E-mail: twoolf@welchlink.welch.jhu.edu.



0006-3495/97/11/2376/17 $2.00

extension of this method to other systems has been used for simulations of the pf1 coat protein and a designed α-helix [Roux and Woolf, 1996; Belohork et al., 1997 (submitted)]. A comparison of the same method applied to a large set of peptides has not been presented.

Bacteriorhodopsin has been used as a model system for protein structure prediction and for understanding the thermodynamics of membrane protein assembly (see Fig. 1) (Lozier et al., 1975; Engelman et al., 1986; Rees et al., 1989; Cramer et al., 1992). Studies have shown that the helices of bacteriorhodopsin are capable of independently assembling to form the final, functional, complex (Cherry et al., 1978; Kahn and Engelman, 1992; Kahn et al., 1992). This provides support for the two-stage model of membrane protein folding (Popot and Engelman, 1990). The two-stage model of folding posits a thermodynamic stage of protein assembly with independent α-helices within the plane of the bilayer. The interaction of these helices with each other then drives the final assembly into a functional protein. This suggests that an understanding of the motions, structures, and interactions of the bacteriorhodopsin helices with the bilayer would be instructive for the thermodynamics of membrane protein structure determination. Table 1 shows the primary sequences of bacteriorhodopsin and further breakdown into different residue types found within each of the seven helices. Recent work with other membrane proteins has suggested that, similarly to globular proteins, an extensive network of protein machinery exists to aid the folding process (e.g., Do et al., 1996; Rapoport et al., 1996). Nonetheless, it is clear from the experiments with bacteriorhodopsin that thermodynamics alone can fold certain membrane proteins into a functional form.

The prediction of membrane protein tertiary structures is being pursued in several labs (e.g., Treutlein et al., 1992; Baldwin, 1993; Cronet et al., 1993; Taylor et al., 1994; Tuffery et al., 1994; Adams et al., 1995; Herzyk and Hubbard, 1995; Sansom et al., 1995; Suwa et al., 1995). The current approach, in all cases, concentrates on helix:helix interactions and neglects the membrane environment. This assumption may, ultimately, prove to be reasonable. But the validity has not been proven by calculations of the relative strength of helix:lipid versus helix:helix interactions within the plane of the bilayer. The analogous situation for globular proteins has shown that the inclusion of solvent does change the energy surface for folding (e.g., Brooks et al., 1988). For example, it has been shown that the rational discrimination of misfolded globular proteins depends on the inclusion of water (Novotny et al., 1984). It would not be surprising, then, to discover that a more accurate potential energy surface for prediction of membrane protein folding requires consideration of the solvent environment.

This paper presents calculations using the CHARMm molecular dynamics program for 10 α-helix/DMPC simulations. In each case the central α-helix is surrounded by 12 lipid molecules in a periodic hexagonal array within the bilayer plane. Further periodic boundary conditions in the direction orthogonal to the plane with TIP3 water caps provides an effectively infinite multilayer system representative of a liquid crystalline environment. The protocol for each simulation consisted of 100 ps of equilibration and at

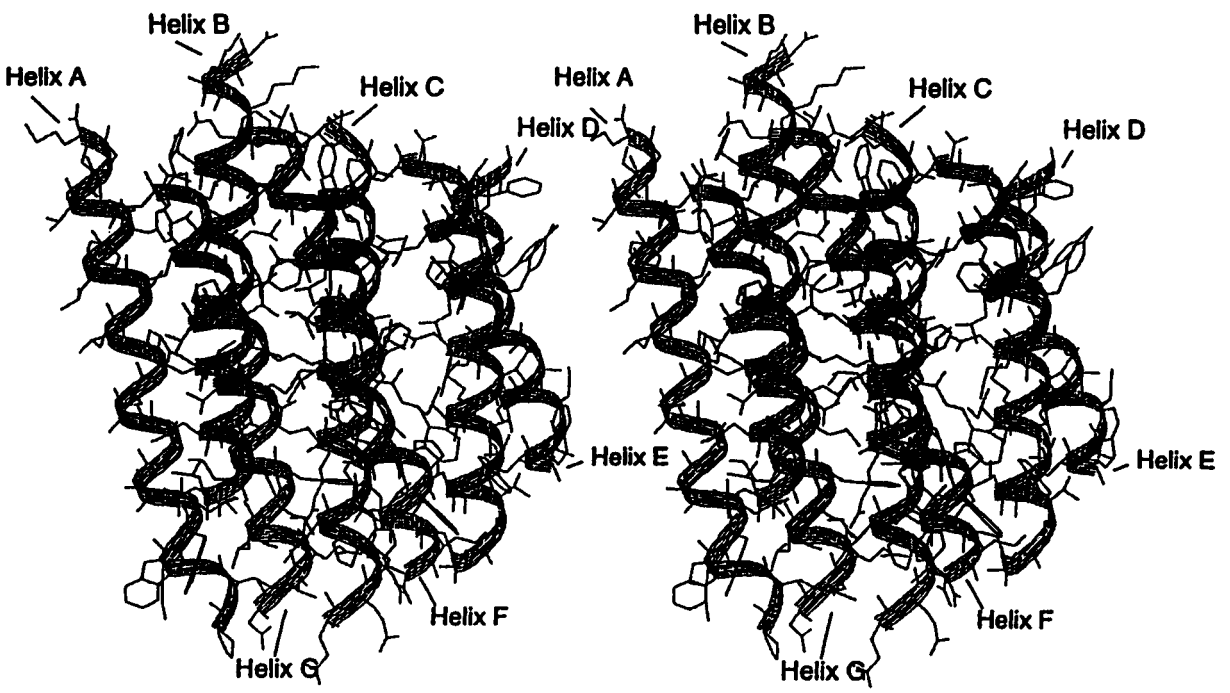


FIGURE 1 Stereo pair of bacteriorhodopsin structure. The α-helices are shown in ribbon representation and are labeled. The structure was determined by Henderson et al. (1990) via electron diffraction and is 3.5 Å resolution in the bilayer plane and 10.0 Å perpendicular to the bilayer.

**TABLE 1 Bacteriorhodopsin helical sequences**

```
A:      TRP ILE TRP LEU ALA LEU GLY THR ALA LEU MET GLY LEU GLY THR LEU TYR PHE LEU VAL LYS GLY MET
B: ASP ALA LYS LYS PHE TYR ALA ILE THR THR LEU VAL PRO ALA ILE ALA PHE THR MET TYR LEU SER MET LEU LEU
C:              TRP ALA ARG TYR ALA ASP TRP LEU PHE THR THR PRO LEU LEU LEU LEU ASP LEU ALA LEU LEU
D:              ILE LEU ALA LEU VAL GLY ALA ASP GLY ILE MET ILE GLY THR GLY LEU VAL GLY ALA LEU
E:      TRP TRP ALA ILE SER THR ALA ALA MET LEU TYR ILE LEU TYR VAL LEU PHE PHE GLY PHE THR
F: VAL ALA SER THR PHE LYS VAL LEU ARG ASN VAL THR VAL VAL LEU TRP SER ALA TYR PRO VAL VAL TRP LEU ILE
G:      ILE GLU THR LEU LEU PHE MET VAL LEU ASP VAL SER ALA LYS VAL GLY PHE GLY LEU ILE LEU LEU ARG
```

Aromatics

- TRP
  - Helix A 1,3
  - Helix C 1, 7
  - Helix E 1, 2
  - Helix F 16, 23
- TYR
  - Helix A 17
  - Helix B 6, 20
  - Helix C 4
  - Helix E 11, 14
  - Helix F 19
- PHE
  - Helix A 18
  - Helix B 5, 17
  - Helix C 9
  - Helix E 17, 18, 20
  - Helix F 5
  - Helix G 6, 17

Charges

- ASP
  - Helix B 1
  - Helix C 6, 17
  - Helix D 8
  - Helix G 10
- GLU
  - Helix G 2
- ARG
  - Helix C 3
  - Helix F 9
  - Helix G 23
- LYS
  - Helix A 21
  - Helix B 3, 4
  - Helix F 6
  - Helix G 14

Prolines

- PRO
  - Helix B 13
  - Helix C 12
  - Helix F 20

least 250 ps of dynamics. Two simulations were extended for an additional 250 ps for a total of 500 ps. In total, the 10 simulations and their equilibration represent a sum of 4 ns of computer time. The present paper analyzes the trajectories for structural and dynamical properties. A second paper (Woolf, 1997, submitted), further analyzes the 10 simulations in terms of interaction energies. Preliminary results from the simulations have been presented (Woolf, 1996).

## MATERIALS AND METHODS

### Initial structures

The Henderson et al. model (1990) (see Fig. 1; 1BRD) provided the starting point for each individual α-helix (Henderson et al., 1990). The α-helices were extracted from the Brookhaven Protein Data Bank entry and each helix was aligned with its axis normal to the bilayer. The more recently refined bacteriorhodopsin structure (Grigorieff et al., 1996; 2BRD) was not available at the time the simulations of this paper were completed (Fall, 1995). The differences in the α-helix starting points (as judged by the paper) are minimal. It could be argued that an equally plausible beginning point for the simulations would have been a set of canonical α-helices with the bacteriorhodopsin primary structure. Such a starting point would have provided an interesting comparison with the current simulations, but running another set of 10 simulations with a different starting point would have required a considerable expense of CPU time. It is not clear that the gain in knowledge from consideration of multiple possible starting points for the 10 simulations would have offset the cost in computer time. A similar starting point (from the x-ray crystal structure) has been used for simulations of isolated myoglobin α-helices in water (e.g., Soman et al., 1991; Hirst and Brooks, 1995).

### Simulations

The simulations used the NVE (microcanonical) ensemble. This choice of simulation system requires an estimate for the lateral square area for each α-helix and DMPC lipid to set the pressure. The α-helical cross-sectional area was estimated from the CHARMm subroutine coor surface. This routine determines the cross-sectional area within a user-defined grid. Previous simulations of the gramicidin A channel in a DMPC bilayer showed that this estimate of the cross-sectional area was reasonable (Woolf and Roux, 1994, 1996). A value of 64 $Å^2$ for the DMPC cross-section was used. This value is considered the current best estimate for this parameter (Nagle, 1993). After these simulations were nearly completed, the possibility of repeating the simulations with constant pressure algorithms became an option (Feller et al., 1995; Zhang et al., 1995). The constant pressure algorithms require the choice of a surface tension term in addition to the normal pressure and adjust the box size during the simulation to maintain pressure and tension constant. There is currently some debate as to the best choices to use for these parameters (Chiu et al., 1995; Feller and Pastor, 1996; Jahnig, 1996; Roux, 1996; Tu et al., 1995, 1996). Simulations are currently being performed with this new constant pressure algorithm and the results will be compared with the current results for a subset of α-helices in a later publication.

The initial placement, and construction of the starting point for dynamics, of the lipids around the α-helix is critical for reasonable relaxation of the system during equilibration. This is likely to be especially important for large, heterogeneous membrane proteins (Woolf and Roux, 1994, 1996). To begin the current simulations, an initial choice for the placement of the lipids was determined by a 500-ps simulation of large vdW spheres to simulate the DMPC headgroups. The α-helix was kept rigid. The spheres were confined to planes surrounding the phosphate region of the eventual bilayer. This created a set of initial placements for the lipids that is responsive to the distribution of side chains and shape of the α-helix. The set of 12 initial positions were then used for placement of the DMPC phosphate atoms. The same method was used for Gramicidin A/DMPC simulations (Woolf and Roux, 1994, 1996). A set of 2000 DMPC lipid conformations provided by Pastor and co-workers was used to initiate the simulations from conformers representative of the liquid crystalline state (Hardy and Pastor, 1994). This supports a more rapid relaxation than would a start from an all-*trans* conformation (e.g., see Heller et al., 1993). Other methods have been used for the generation of starting structures for detailed molecular dynamics computer calculations. For example, Stouch's group gradually grew in an awareness of the protein through an increasing

**TABLE 2 Molecular dynamics calculations**

| Helix A | Helix B | Helix C | Helix D | Helix E | Helix F | Helix G |
|---|---|---|---|---|---|---|
| 250 ps | 250 ps<br>250 ps (charged) | 500 ps<br>500 ps (charged) | 250 ps<br>250 ps (charged) | 250 ps | 250 ps | 250 ps |

volume in the center of the simulation cell containing pure lipid (Shen et al., 1996).

The lipids were systematically rotated and translated to cut down on the number of bad contacts. A bad contact was defined as heavy atoms within 2.6 Å of one another. Following the systematic rotations and translations, a gradual awareness of neighboring atoms was grown into the system by using a series of short cutoff distances for nonbonded interactions. A TIP3 water overlay was performed from the glycerol regions on both sides to support a z-periodicity of ~70 Å. The final number of atoms in the systems was near 4000. Equilibration dynamics was pursued with a gradually decreasing series of harmonic restraints. The first 25 ps of dynamics used a 1.0 kcal/mol-Å$^2$ restraint on all heavy atoms and Langevin dynamics with a collision frequency of 5/ps. This low value for the collision frequency has been shown to maximally allow for relaxation of the system while providing a temperature coupling to the heatbath (Loncharich et al., 1992). The next 25 ps used velocity scaling with no restraints on atom positions. This was followed by 50 ps of no restraints and no temperature coupling. The temperature remained constant throughout the simulation of each system.

The nonbonded list was cut at 12 Å with electrostatics shifted and vdW interactions switched. The vdW interactions used a switching region of 4 Å. The list was generated to 14 Å and an automatic update of the nonbonded interactions was performed if the deviations exceeded 1 Å. Atom-based cutoffs were used. This has been shown to produce reasonable results with the CHARMm parameter function from previous simulations (Venable et al., 1993; Woolf and Roux, 1994, 1996). Other investigators have used a group-based cutoff with good results (Bassolino-Klimas et al., 1993; Shen et al., 1996). The empirical potential function developed in the Karplus group was used (Schlenkrich et al., 1996).

Conformations were saved every 50 fs throughout the time from 100 ps to 350 ps for eight simulations. Two simulations were extended from 350 ps to 600 ps with the same rate for saving conformations. In all cases, the SHAKE algorithm was used with a time-step of 2 fs. Further details of analysis and construction can be found in other recent papers that used this approach (Woolf and Roux, 1994, 1996; Roux and Woolf, 1996; Belohork et al., 1997, submitted). The simulations of this paper, on average, required 1.8 CPU h/ps on a SGI R4400 machine. Due to time sharing on the machines, the actual time for each simulation was several months.

Analysis used the CHARMm subroutines and FORTRAN programs written specially for the current simulations.

## RESULTS AND DISCUSSION

The microscopic details of helix:bilayer interaction were examined by 10 simulations of individual α-helices from bacteriorhodopsin. This allowed a detailed cross-comparison of simulations with the main difference between simulations being limited to the central α-helix. Table 2 lists the 10 simulations and their total simulation length. The simulations used identical simulation environments, potential functions, construction, and equilibration protocols. The differences in calculated motional behavior and average structure are related to the different primary sequences of the helices. Six simulations were performed for helices B, C, and D with charged and neutral side chains. For helix B this was a change in the charge-state of the lysine side chains at positions 2 and 4. For helix C, this was a change in the aspartate charge state at positions 6 and 17. For helix D, the aspartate charge at position 8 was changed.

The molecular dynamics simulation environment is illustrated as a stereo pair in Fig. 2. The central simulation cell was hexagonal in shape and periodic boundary conditions were applied both within the plane of the bilayer and normal to the bilayer. The resulting system is representative of an oriented liquid-crystalline multibilayer.

The subsections to follow will describe the individual figures with some discussion of context for each result. The concluding discussion will bring together all the figures and tables and further discuss the 10 simulations.

### Root-mean-squared deviations from trajectory-averaged structure

The root-mean-squared (rms) deviations from a reference or average structure provide evidence for the extent of motional types present in a simulation. An important result from the present simulation is that not all the helices had the same types of motion within the bilayer. This is strikingly seen in Fig. 3, where the rms deviations from the trajectory-averaged structure is presented for all 10 simulations. The time-averaged structure is determined as an average of all

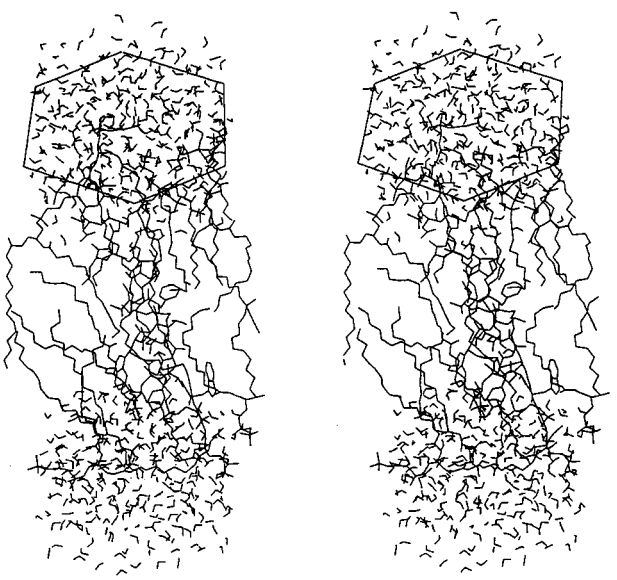

FIGURE 2 A: Stereo pair of the central simulation cell. Periodic images were used to make an effectively infinite multilayer system. A hexagon is drawn over the system at the level of the DMPC headgroups to provide a visual sense of the central cell. Only heavy atoms of the protein and lipid are presented.

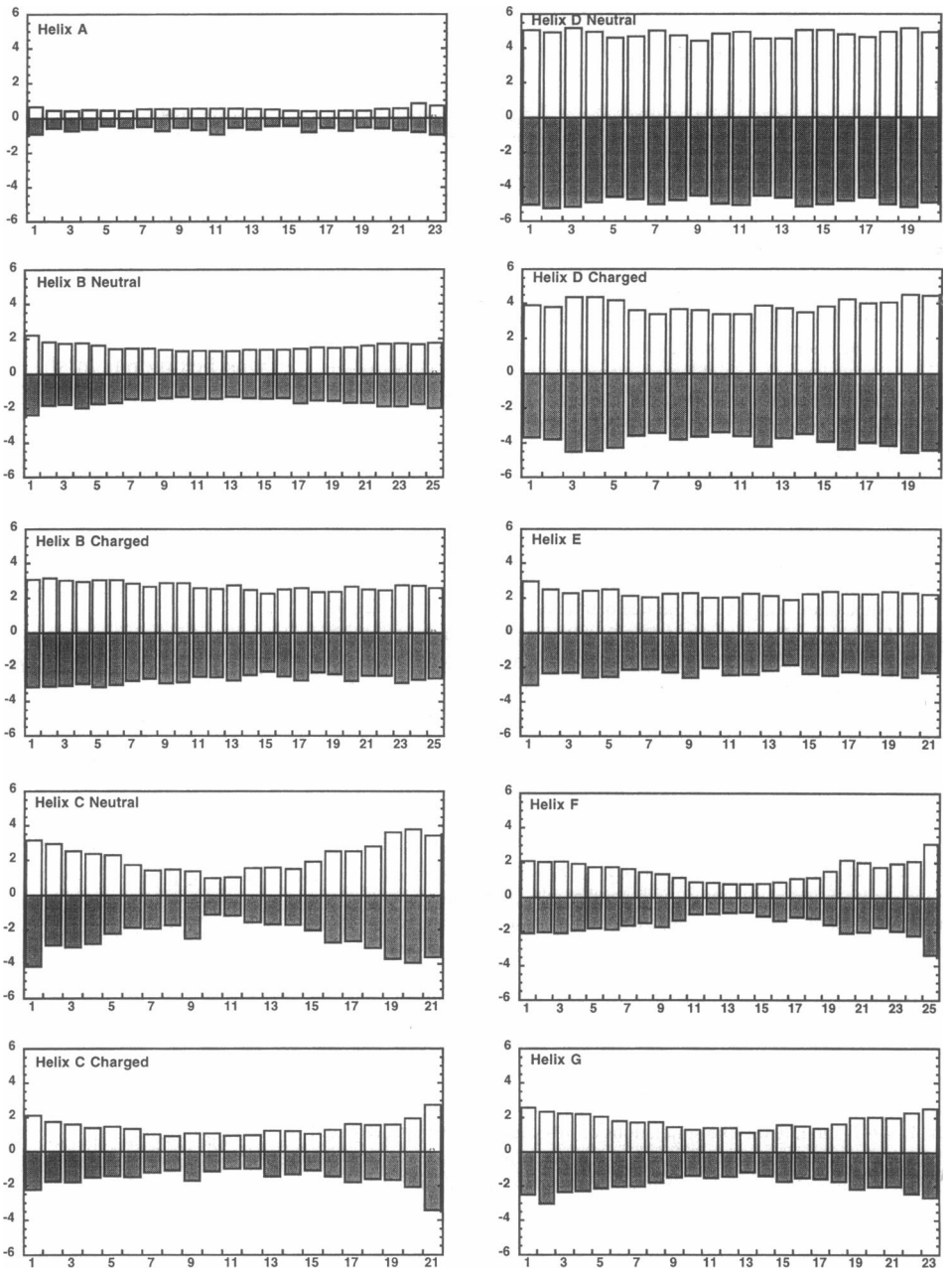


FIGURE 3 RMS deviations from the trajectory-averaged structure. The positive white-filled bars represent deviations of C-$\alpha$ atoms from the average structure. The gray-filled negative bars represent rms deviations of all heavy atoms from the average structure. The average structure was determined from the full trajectory for each $\alpha$-helix.

conformations over each full trajectory. The rms deviations for helix A is on the order of 1.0 Å. In contrast, the rms deviations for helix D are on the order of 4.0 Å. The large change in rms is spread throughout the length of the helix for both of these peptides. Another type of motional behavior is suggested by helices C, F, and G. In these three helices, the mobility is greater near the ends of the helix than near the center of the bilayer. In each case, the figure shows the C-$\alpha$-rms deviations as a white box going up and the all-heavy atom rms deviations as a gray box projecting down. The horizontal axis is the residue number.

The rms deviations can differ between charged and neutral helices. For example, helix B-charged has greater fluctuations than helix B-neutral. In contrast, helix C-neutral has larger fluctuations at the ends than helix C-charged, but has similar fluctuations at the center for both cases. Helix D has similarly large fluctuations for both charged and neutral forms. The neutral form of helix D has slightly larger fluctuations than the charged form.

## Backbone dihedral angles

A rigid $\alpha$-helix would remain with set phi-psi angles throughout a molecular dynamics simulation. In contrast a flexible chain with little restriction to a particular secondary structure would frequently deviate from a regular $\alpha$-helix during a trajectory. To examine the motional restrictions on

the backbone dihedrals, the mean and the rms deviations of the backbone phi-psi angles of each helix were calculated from the production trajectories. The results show differences between the helices with most of the helices adopting a mean structure that remained α-helical.

Fig. 4 shows these average and rms deviations of phi-psi angles. The psi angles were multiplied by −1.0 to enable both sets of data to be present on a single plot. The gray bars represent the average value of the dihedral averaged over the simulation trajectory. The white bars at the tips of the averages reflect the size of the fluctuations from the mean as measured with a standard deviation. Only the positive rms deflection is indicated. The values of these dihedrals can be compared with the usual (phi, psi) values for an α-helix of (−47,−49) for a π-helix of (−70,−57) and of (−26,−49) for a 3–10 helix (Creighton, 1993). The fluctuations from the average varied from helix to helix. The largest fluctuations are seen for the neutral helix D simulation.

Not all the structures retained full α-helical phi-psi angles throughout the simulation. Partial unwinding was observed at the ends of the charged simulations for helices C and D. Note that the change in some vertical scales makes it appear

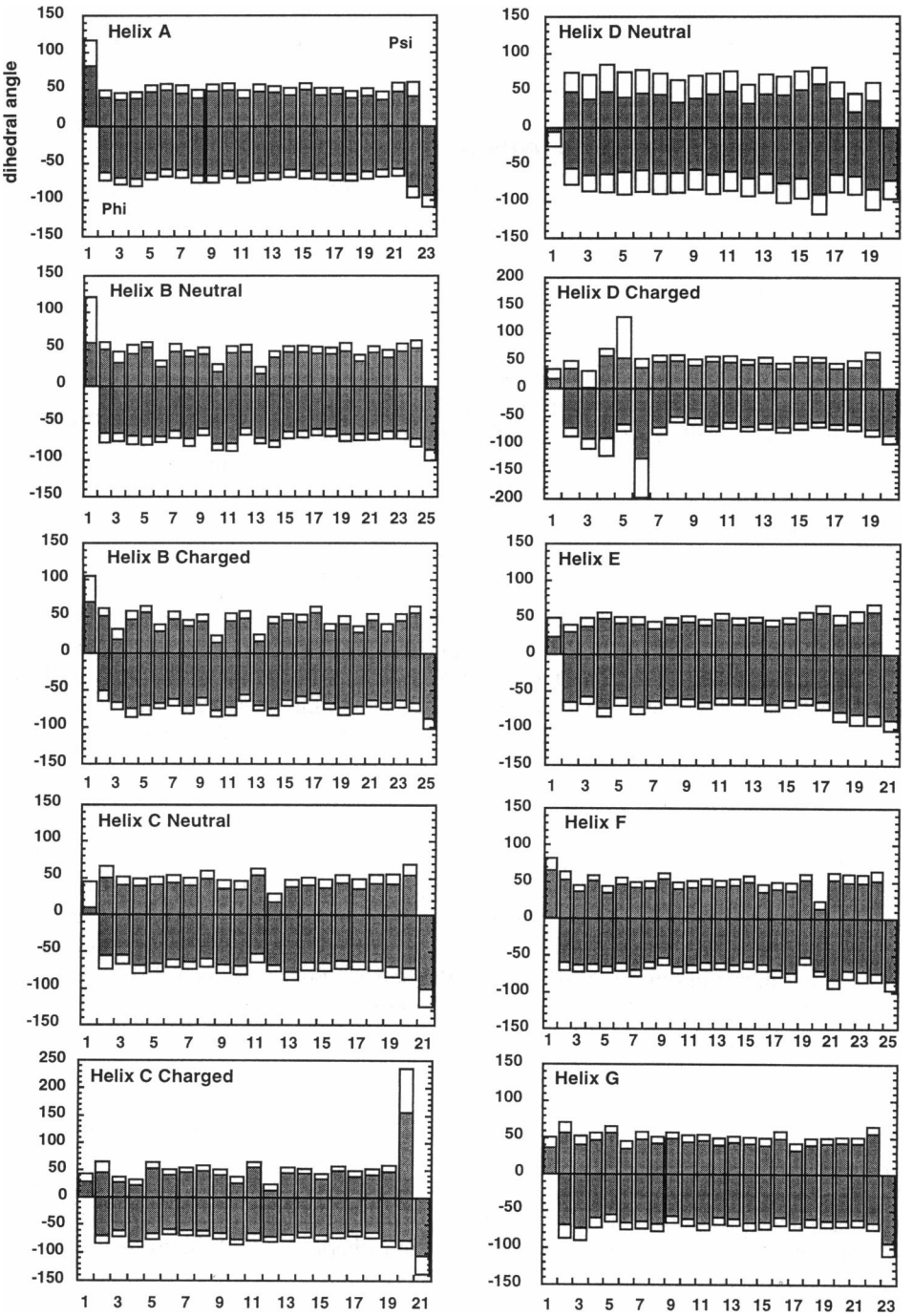


FIGURE 4 Phi/Psi backbone dihedral angles for each of the 10 simulations. The psi values have been multiplied by −1 to allow presentation of both sets of angles on a single plot. The gray bars present the average value for the dihedral angle. The white tips give the rms deviations observed in the trajectory. Note the changes between helix A and helix D.

that there is a larger change with helix D-charged and helix C-charged than is actually the case. In the example of helix D-charged, the region from residues 8 to 20 remained as an $\alpha$-helix, while the region from 1–7 became partially unwound. Helix C-charged was partially unwound from residues 19 to 21, while residues 1 to 18 remained stable.

These results indicate that the $\alpha$-helix secondary structure remained a relatively stable constant of simulations for 8 of the 10 simulations and was relatively less stable for two simulations at parts of the helix. This gives an indication of the complexity of coupling between helical motions and the environment. For example, the greater fluctuations from the $\alpha$-helical values evidenced by helix D-neutral can be compared with the smaller fluctuations from the same set of values for helix A.

## Backbone hydrogen bonding pattern

A distinguishing feature of regular $\alpha$-helical secondary structure is the presence of i:i + 4 hydrogen bonding patterns along the length of the helix. Deviations from this hydrogen bonding pattern can occur to i:i + 3 and i:i + 5 hydrogen bonding interactions for the 3–10 and $\pi$ helices. An analysis of the types of hydrogen bonding interactions occurring during the simulations thus gives insight into the relative stability of different secondary structural motifs.

Fig. 5 shows the lifetime and type of hydrogen bonding observed during the full simulation for each of the 10 helices. The i:i + 4 hydrogen bonding pattern was the predominant form observed in each case. Additional i:i + 3 and i:i + 5 hydrogen bonding patterns were observed in some of the helices. The criteria for presence of a hydrogen bond was the value of the O—N distance. A distance <3.0 Å was considered to be reflective of a hydrogen bond, while distances greater than this number were considered indicative of a lack of the particular type of hydrogen bonding pattern. No angle criteria were used. For each type of hydrogen bond, the total percent of time during the simulation that a particular distance cutoff was met is presented in the figure. The dark fill pattern is to indicate the i:i + 4 canonical hydrogen bonding typical of an $\alpha$-helix. The medium-light fill pattern is an i:i + 3 hydrogen bonding pattern, and the i:i + 5 hydrogen bonding is shown in the lightest fill pattern.

There are intriguing differences between the helices. For example, helices A and G had a relatively high percentages of time spent in the i:i + 4 hydrogen bonding pattern. Helix B, for both charged and neutral trajectories, had a higher percentage of i:i + 4 hydrogen bonding from residues 12 to 22 compared to earlier residues. Helices E and F had a mix of satisfied and unsatisfied hydrogen bonds along the length of the helix. In the case of helix E, an i:i + 5 hydrogen bonding pattern was observed for residues 15:20 and 16:21 for part of the trajectory. Helices C-neutral and charged were i:i + 4 hydrogen bonding for two separate sections of the helix. Helix C-neutral had a higher percentage of hydrogen bonding of the i:i + 4 type than did the charged variant. Helix D-neutral had a much higher i:i + 4 pattern of hydrogen bonding for residues 1 to 6 than did helix D-charged.

The observed differences in hydrogen bonding patterns (Fig. 5) are reflective of the motional behavior determined by the lipid environment and the primary sequence on the helix. The breakdown of i:i + 4 hydrogen bonding does not necessarily mean that the helix structure itself is broken, only that the hydrogen bond is not present for a percentage of time during the simulation. The presence/absence of the hydrogen bonds may be related to motional coupling between the side chains and the lipid environment coupled into the backbone. A side chain that is strongly coupled to the environment to the exclusion of a residue i + 4 distant that has a weaker coupling could lead to a situation with less time-averaged satisfaction of the hydrogen bond than a situation where both side chain residues are equally strongly coupled to the environment. This also illustrates a potential problem with vacuum and uniform media simulations as analogs of the lipid bilayer for isolated membrane protein helices. Such simulations implicitly assume that the environment has the same coupling to all side chains regardless of position within the bilayer system and side chain type.

## Lipid conformations

The percent of *gauche* conformations in the lipid alkane chains was calculated in two different ways. A first method averaged over all 12 lipids and discriminated between the sn1 and the sn2 chains. The second method averaged the total percent *gauche* in both chains for each lipid.

The percent *gauche* using the first method is portrayed in the results of Fig. 6 *A*. The percentage for the sn2 chain is multiplied by $-1.0$ to enable both sets of data to be presented. The dark fill lines are the percent *trans*, while the two lighter fill types are the percent *gauche*$^+$ and *gauche*$^-$. If the simulations converged the two *gauche* populations should be equal. The figure can be analyzed by comparing overall trends for *gauche* between the different helices, as well as the differences for particular chain positions between helices. For example, the ninth chain position for the charged helix B simulation has a much lower percent *gauche* in both chains relative to the same position for the other helices. In all cases, the first chain position is more likely to be *gauche*. This is expected for a position near the glycerol group.

The second method is presented in Fig. 6 *B*. The results show differences between lipid states surrounding the helices. For example, helix C-neutral shows a nearly uniform distribution of percent *gauche* conformations throughout the lipid population. In the case of helix A, the percent *gauche* conformation varies from 10 to 30 percent in comparing the 7th lipid with the 1st or 8th lipids. This is related to preferred conformations adopted by the lipids in response to the presence of the helix.

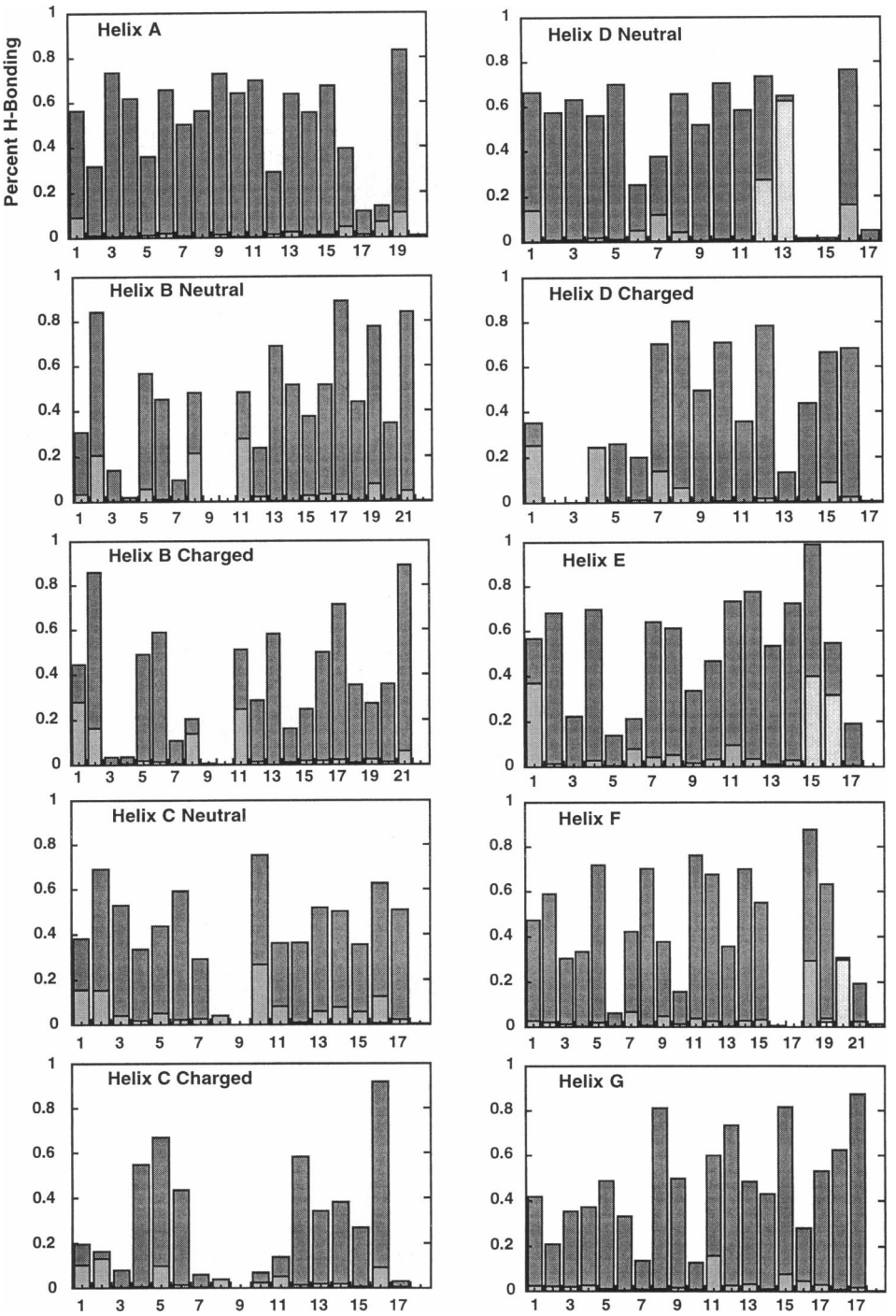


FIGURE 5 Backbone hydrogen bonding patterns. The distance between O and N atoms was used as the criteria for presence of a hydrogen bond. If this distance was <3.0 Å the conformation was counted as a particular type of hydrogen bond. No angle restrictions were used for identification. For each of the 10 simulations, the percent of time for a particular type of hydrogen bond is indicated. The darkest fill pattern is a i:i + 4 hydrogen bond, the medium fill pattern is a i:i + 3 type of hydrogen bond, and the i:i + 5 bonding pattern is indicated in the lightest fill pattern.

## Rigid body motion

An important variable for the overall folding of a membrane protein is the relative mobility of each helical subunit in the lipid bilayer. Are the subunits best thought of as locally rigid bodies without internal motion or is the internal motion an integral part of their behavior? The ability to think of the α-helical subunits as relatively rigid bodies would be a great aid to tertiary structure prediction.

To quantitatively examine the dynamical motion of subparts of each helix, an overlapping series of best-fit cylinders to eight residue main-chain atoms was determined. The cylinder axis was compared with the normal to the bilayer ($z$ axis). This analysis gives insight into whether the α-helix moves as a single rigid body or with more complex independent sets of subdomains. Fig. 7 illustrates the time dependence of the tilt angle for the 8-residue cylindrical subsets for each of the 10 simulations. There are considerable differences in behavior from one helix to another.

To enable visualization and comparison of the different best-fit cylinders within a helix and between the helices, the $y$ axis of the plots is not a true displacement scale: an

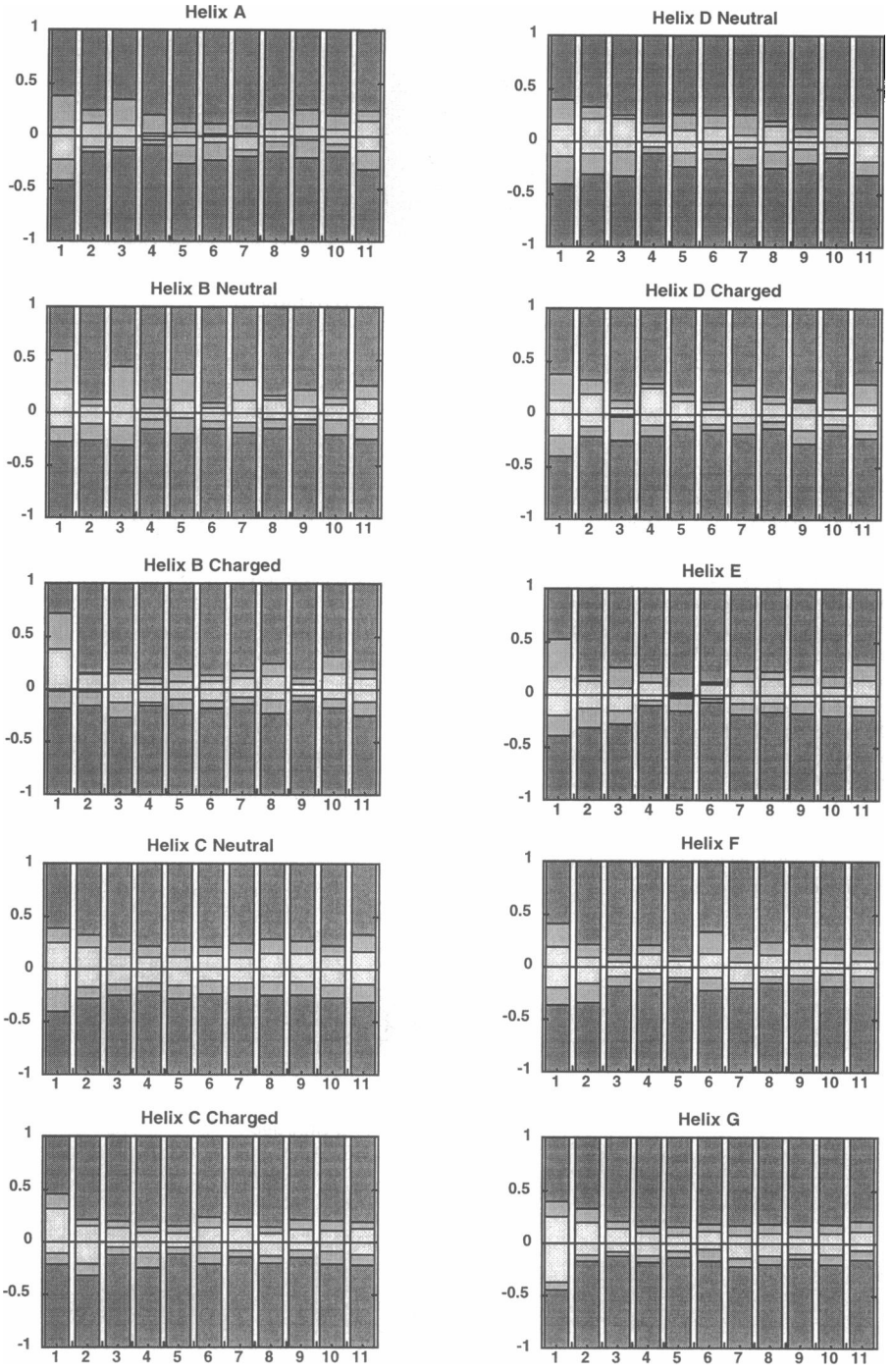


FIGURE 6 Lipid conformations as averages over the trajectory for all 10 simulations. (*A*) shows a breakdown along the two alkane chains averaged over all 12 lipids. The positive deflection is sn1, the negative is sn2. The dark fill is percent of time in the *trans* conformation, the medium and light fills represent percent of time in the two *gauche* states. (*B*) presents the percent *trans*, *gauche*$^+$ and *gauche*$^-$ as a function of lipid number. The percentages are averaged over both alkane chains and all dihedrals for each lipid.

arbitrary displacement was added to each subsequent time series to enable a vertical separation. The 20° displacement bar on the left of the figure should be used as a guide to the size of the fluctuations. This method gives an immediate sense for the differences in 8-residue cylindrical movements.

Helix A has the smallest set of fluctuations and helix D the largest. Helices C-charged, C-neutral, and F show evidence of two separate domains of motion. There is also some evidence of different subdomains in helix D-charged. Helices A, B-charged, B-neutral, D-neutral, E, and G all show motional behavior similar to a rigid single domain. The presence of a proline residue in helices C and F provides a structural basis for the two motional domains. The proline in helix B does not appear to introduce a break in the motional behavior of the cylindrical subsets across the bilayer.

To further examine the motional behavior of the cylindrical domains separated by the proline, two cylinders were best fit on each side of the proline residue for helices B, C, and F. As a check, helix A was also divided into two cylinders for analysis. The results illustrated that helices C and F have larger fluctuations in tilt angle between the two domains than helices A and B. This is illustrated for the case

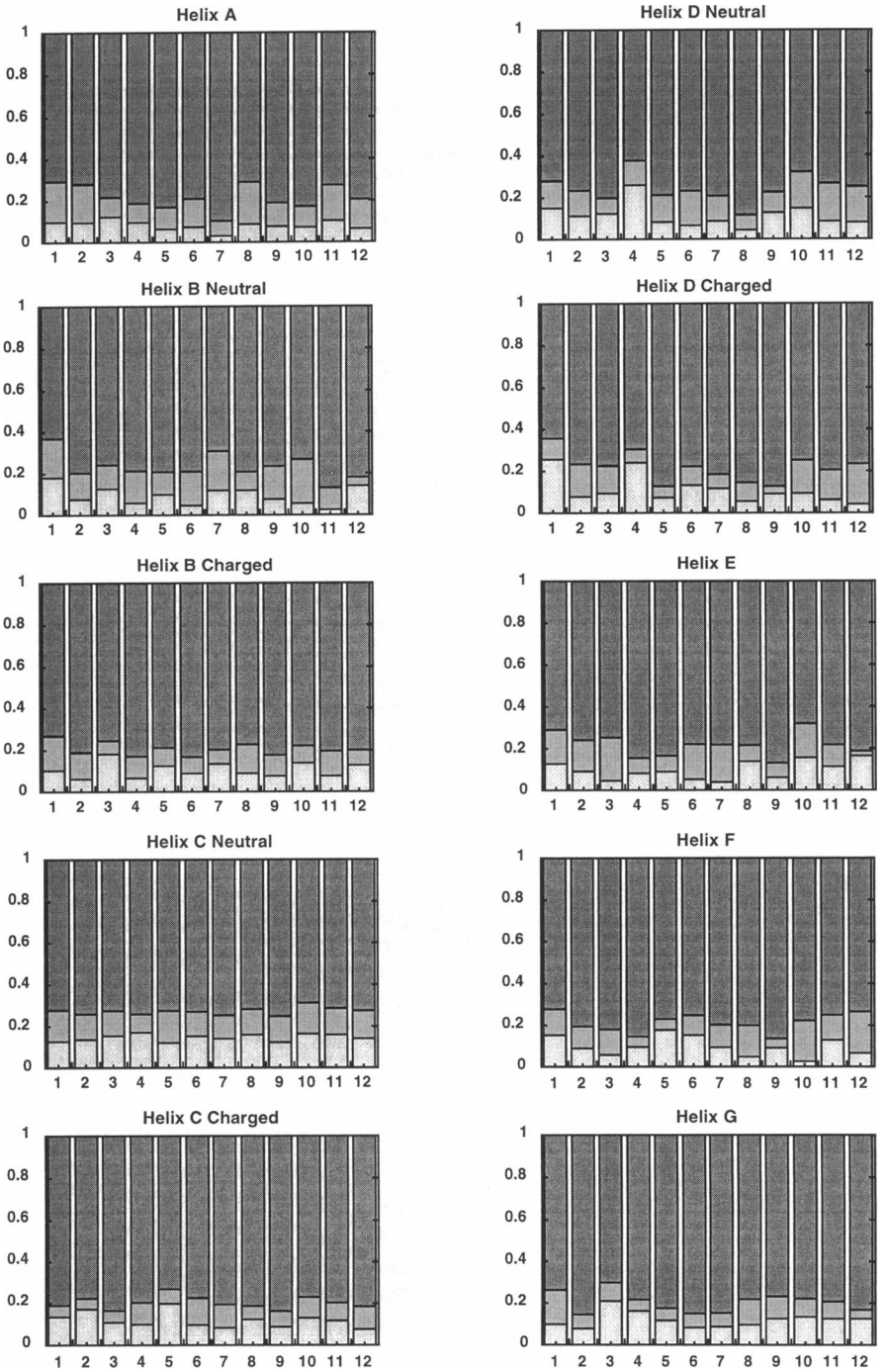


Figure 6. *Continued.*

of helix A versus helix C in Fig. 8. This type of analysis further confirms that it is possible to think of the proline residue as creating a separation between two separate domains of motion for helices C and F.

This last result suggests that a division into separate domains of α-helical secondary structure may be associated with the presence of a proline residue. This is related to speculation about the possible functional roles of proline residues in membrane proteins (Deber et al., 1990a,b; Williams and Deber, 1991; Heijne, 1991). It is also similar to results for isolated α-helices in vacuum that suggested greater motional change about a hinge-axis (Sankararamakrishnan et al., 1991; Sankararamakrishnan and Vishveshwara, 1990, 1992, 1993; Sansom, 1992; Breed et al., 1995; Sankararamakrishnan and Sansom, 1994) and to simulation results for single proline containing α-helices in explicit water (Yun et al., 1991). The result further suggests that the proline residues can be thought of as local helical hinge-points allowing two separate relatively rigid bodies to be functionally separated. This may be further related to

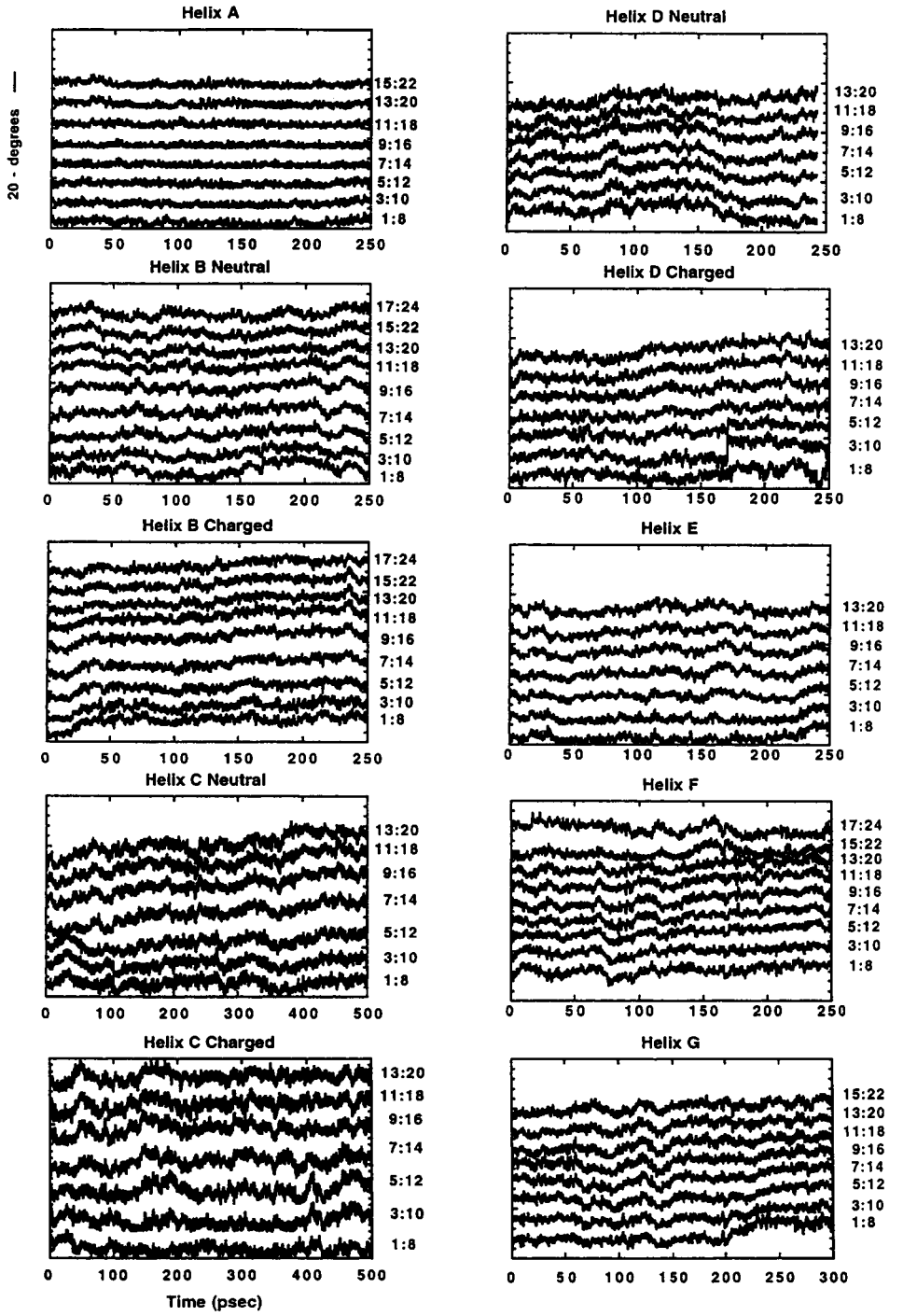


FIGURE 7 The motional behavior of eight residue subsets of each helix considered as a cylinder. The best-fit cylinder for sets of eight residue backbone atoms was determined at each time point. The angle between the cylinder axis and the bilayer normal is plotted for each cylindrical subunit. An arbitrary displacement along the $y$ axis was used to enable presentation of all sets of cylinder time-courses on the same series of plots. The scale bar should be consulted for a 20° vertical fluctuation. The numbers to the right of each curve label the residues contained in the cylinder.

observed structural changes in the M-stage of the bacteriorhodopsin photocycle (Subramaniam et al., 1993).

## Side-chain dynamics

The character of the solvent environment is expected to influence the torsional barriers for side-chain dynamics. Thus, while a detailed comparison was not made, the current simulations will differ from simulations of the same set of helices within a homogeneous solvent. To investigate the effect of position on side-chain dynamics, the trajectories were analyzed in terms of the average and rms deviations from the average for all chi-1 and chi-2 values of all side chains in all 10 simulations. The results are partially shown in Fig. 9. In particular, the figure shows the chi-1 averages and rms deviations as a function of relative bilayer distance for three different amino acid types pooled together from all 10 simulations.

Several interesting results are obvious from Fig. 9. First, for chi-1 in Leu, the majority of side chains are found in the

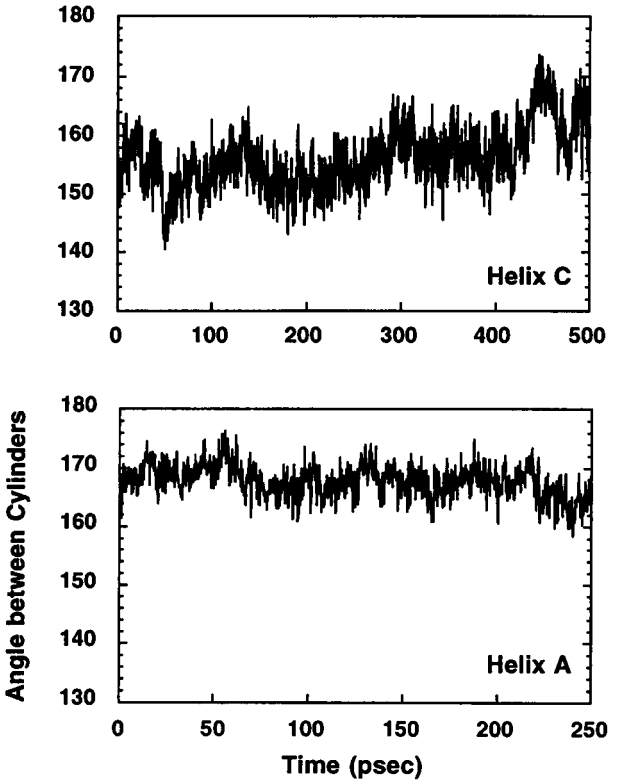


FIGURE 8 The angle between two helical axes defined by proline in helix C and for comparison the same type of angle between two cylinders at the middle of helix A. The motions observed for two of the three proline-containing helices were larger than that observed for the nonproline-containing helices.

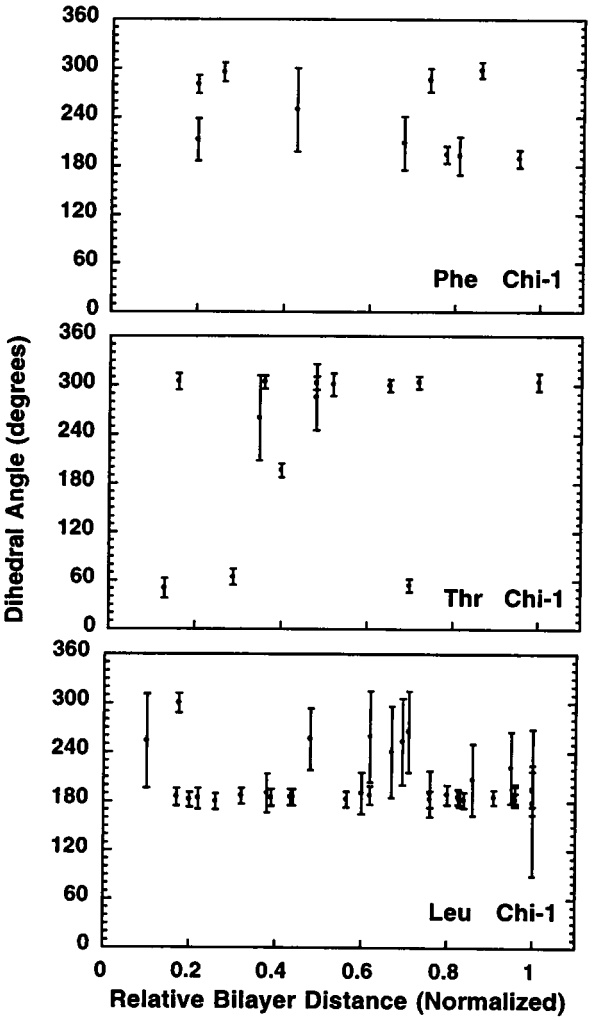


FIGURE 9 Side chain chi-1 for selected amino acid residues. The plot uses a normalized effective distance across the bilayer by scaling the number of amino acids as a function of the total number in the helix. The average and rms deviations are shown for time-series calculated from the full trajectory.

*trans* state with relatively small rms deviations throughout the full trajectory. In contrast, the *gauche* conformers have a much larger rms deviation over the trajectory. Secondly, not all the Thr and Ser side chains remained hydrogen-bonded to the backbone carbonyl oxygens throughout the trajectories. Considerations of crystal structures suggested that Cys, Ser, and Thr side chains may predominately satisfy hydrogen bonding with the internal backbone carbonyls, and therefore not find the bilayer interior a disfavored environment (Gray and Matthews, 1984). The simulation results suggest that there is not a strong energetic driving force to maintain internal hydrogen bonding. In fact, the majority of chi-1 values for Ser and Thr in the middle of the bilayer indicate a lack of internal hydrogen bonding. This is in contrast to the Ser/Thr near the interface where the hydrogen bonding interactions are more readily observed.

## Radial distribution functions

Fig. 10 shows the radial distribution functions for the hydrogen-bonding atoms of Trp and Tyr side chains. The presence of these hydrogens and their capacity for forming hydrogen bonds sets these two aromatic residues apart from other types of side chains. In particular, a stable set of hydrogen bonds from these oxygens to the rest of the system may have an effect on the overall rms stability of the system. This is suggested from considering the differences between Trp and Tyr side chains on different helices. For example, the reason that helix E is not as stable as helix A may be traced to the hydrogen-bonding pattern of the aromatics of helix E relative to those of helix A. A priori, it might have been expected that helix E would be equally as stable as helix A, since it has two aromatics at both ends of the helix. But, examination of Fig. 10 shows that for helix E, only one of the four aromatics is consistently hydrogen-bonding throughout the simulation. This suggests that not only the presence of an aromatic, but the surrounding amino acids in the helix, can influence the type of interactions between the protein and the bilayer surrounding.

## Concluding discussion

The present results provide insight into the structural and motional behavior of α-helices within an explicit DMPC

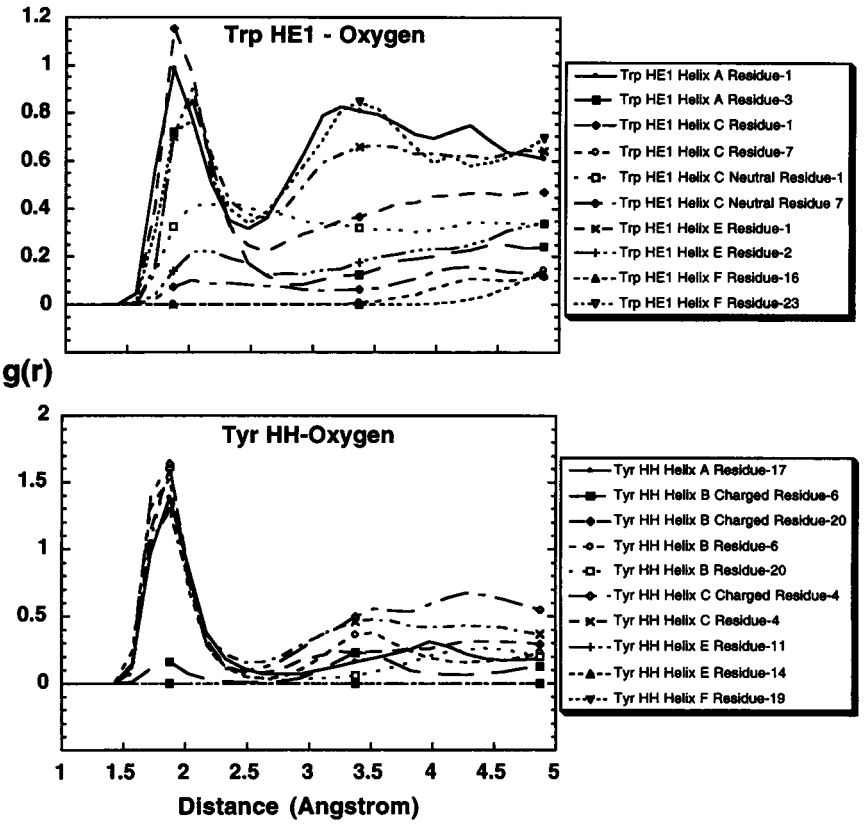


FIGURE 10 The radial distribution function for the oxygens of Trp and Tyr from all 10 simulations. Notice that the hydrogen bonding was satisfied in some of the simulations, but not in all cases. In particular, there are differences between the neutral and charged simulations and between hydrogen-bonding with the side chains at different distances within the bilayer. It is especially interesting to note that for helix A three of three possible hydrogen-bonding interactions at the interface are present through most of the simulation; for helix E, only one of four is present with high probability. This relates to the difference in rms deviations seen over the trajectory for helix A relative to helix E and the other helices.

bilayer. The only significant change between each simulation was the central $\alpha$-helix. Thus, the large differences in motional behavior and in average structural conformation reflect differences in helix interaction with the bilayer environment.

Two types of rigid body motion are observed in the simulations. A first type is evidenced by helices A, D, and E (Fig. 3). The motion is a relatively uniform rms distribution along the helix axis. The second type is evidenced by helices C, F, and G (Fig. 3). This second type is more strongly influenced by rigid-body rotation about a central axis than translational motion for all atoms. This second type of rigid body motion has been discussed in the context of simulations of myoglobin by other researchers (Furois-Corbin et al., 1993). Such independent domains of helical motion could be used to determine the most efficacious methods for determining tertiary structure of membrane proteins. The differences in rms fluctuations between the helices of a given type, e.g., between helices A and D suggests that the internal hydrogen bonding state of the helix (Fig. 5) as well as the coupling of the helix to the lipid environment can have a large effect on the types of motion.

An extensive series of simulations have been performed on proline containing $\alpha$-helices in vacuum (Sankararamakrishnan et al., 1991; Sankararamakrishnan and Visveshwara, 1990, 1992, 1993; Sansom, 1992; Breed et al., 1995; Sankararamakrishnan and Sansom, 1994). One of the central goals of the vacuum simulations was to compare the helices with prolines against those that did not contain proline. The results suggested an increased mobility about a hinge axis determined by the proline. This is consistent with the current results. However, the detailed motional behavior in vacuum is expected to differ from that in an explicit representation of the solvent. Though not compared directly, the current results do differ in the motional dynamics observed. This can be understood as the changes in environment from a nonuniform membrane setting to a homogeneous (vacuum) setting. The membrane environment is a complex mixture of differing chemical types as the surroundings change from the water exterior solution to the alkane interior regions. This change in setting will have an influence on the average structure and dynamics observed in the simulation.

Isolated $\alpha$-helices have been simulated in a variety of explicit solvents (e.g., Hartsough and Merz, 1993; Van Buren and Berendsen, 1993; Kovacs et al., 1995). The results have been analyzed to determine the possible differences in average structural and motional behavior from one environment to another. In water, several of the simulations suggest that an isolated $\alpha$-helix is only marginally stable. In a nonpolar, nonhydrogen-bonding environment, the simulations suggest that the regular secondary structure of the $\alpha$-helix is stabilized. Thus, several simulations suggest that the structure stabilizing effects of certain solvents (e.g., trifluoroethanol) may be due to this effect on hydrogen bonding. The current results, while not compared to similar

calculations in an explicit water environment, do suggest that the membrane environment is more complex in its effects on hydrogen-bonding secondary structure than a homogeneous solvent. In particular, the difference between helix A and helix D suggests that the membrane setting can act to stabilize those types of α-helices that can interact favorably with the interfacial region in contrast to those helices that do not have such strong interactions.

A set of simulations, with the isolated helices of myoglobin (Hirst and Brooks, 1995; Soman et al., 1991), showed that different helices had differential effects with the water environment. The approach of Hirst and Brooks addressed the folding pathway. Such differences in relative stability with the water environment were then related to the formation of larger structures. This is consistent with the overall tone of the current results. Thus, the large differences in motional behavior between helix A and helix D may be related to the thermodynamics of folding. Unfortunately, the folding pathway for bacteriorhodopsin is not known in enough detail for speculation to proceed any further at this date.

The presence of proline has been linked, in globular proteins, to differences in interactions between α-helices (O'Neil and DeGrado, 1990; Hermans et al., 1992). The unusually large effect of a proline on helical dimerization was explained as a change in the relative structures imparted by the proline (Hermans et al., 1992). The other amino acids tended to encourage a particular type of helix:helix interaction that was not present in the helices with a proline at the center. The proline residue was largely understood as creating a change in the effective local flexibility of the helix at the center of the simulation. The series of free energy calculations was effective in providing an explanation for the experimental measurements of changes in helix:helix interaction strength. The molecular dynamics calculations of Hermans et al. also showed that the presence of a proline can create a hinge-point that breaks the helical secondary structure in water. Thus, in analogy to the globular proteins, it might have been predicted that a similar possibility is reached for membrane proteins. Yet, it is not obvious that this would be the case. The membrane environment provides a different set of constraints on motion than the bulk-water environment. A full analysis of this situation would require a set of relative free energy calculations. Such calculations are not unreasonable for the system constructed here, provided that the overall change in bend produced around the proline is not overly large for the simulation cell. It is quite interesting to note that the situation for the three proline-containing helices is not identical. Two of the three helices showed greater motional flexibility around the proline hinge-axis than did the third. This suggests that for a single α-helix in isolation, there may be other factors that contribute to the motional ability.

The presence of proline residues may thus serve to break the helical motion into two independent functional domains. For example, hinge-bending motions important for function have been identified in globular proteins (Gerstein et al., 1993; Holland et al., 1992; McPhalen et al., 1992; Sharff et al., 1992) and suggested in simulations (e.g., Paulsen and Ornstein, 1995). It is possible that the conformational changes observed in helix F during the BR photocycle are related to domains defined by the proline (Subramaniam et al., 1993). However, the three proline-containing helices had differing degrees of motional flexibility. This leads to the suggestion that the ability to adopt "hinge-motions" about the proline axis is not simply related to the proline but is determined also by the presence or absence of aromatic or charged residues. The aromatic or charged residues could change the coupling of the helical domains to the environment. The presence of amino acid types that favor a stable α-helix with well-satisfied internal hydrogen-bonding patterns could also lead to a more rigid structure relative to a situation with a less strongly internally bound helix. Thus, the proline residue alone may not determine the relative hinge-bending ability of the helix. This may be further modulated by helix:helix interactions in the full bacteriorhodopsin structure. This is reinforced by substitution studies from Khorana's lab that suggest replacement of proline does not necessarily disrupt function (Mogi et al., 1989). The time course of the current trajectory, though too short to deduce the details of the relative free energy surface, is strongly suggestive of differences between the three proline-containing helices.

There is a natural wish to relate the current results more directly to the function of bacteriorhodopsin. This is not possible beyond the suggestion that the proline hinge-bending degree of freedom may be important for function. Without considering the interactions between helices, the connection to proton pumping is absent. The results are mainly related to secondary structure prediction and helix/lipid interactions and not related directly to functional considerations in the bacteriorhodopsin system. A recent simulation study of the bacteriorhodopsin trimer in an explicit bilayer environment (Edholm et al., 1995; also Jahnig and Edholm, 1992) and the studies from the Schulten group (e.g., Zhou et al., 1993; Humphrey et al., 1994; Logunov et al., 1995; Xu et al., 1995, 1996) should be consulted for calculations more directly related to bacteriorhodopsin function.

The current results should be understood in the light of the current status of membrane protein molecular dynamics simulations. In particular, these results are the first detailed simulations of a set of α-helices compared within an explicit bilayer environment. The field itself is still very young. For example, the best method to simulate pure lipid bilayers is an active subject of debate (see, e.g., Roux, 1996; Feller and Pastor, 1996; Jahnig, 1996). The current simulations used NVE (microcanonical) simulation conditions. This may not, in the longer-term development of methods, have been the optimal choice. At the time the simulations were initiated, the constant pressure techniques for lipid bilayers had not been developed (Feller et al., 1995; Zhang et al., 1995). Currently, a subset of the helices of the present calculations are being repeated with constant pressure simulations and

the results will be compared with the current results in a future paper.

## CONCLUSION

The microscopic details of protein:lipid interactions are not well understood. By analogy to globular proteins, it is expected that a full analysis of the solvent interactions with protein will be needed to rationally separate misfolded membrane proteins from correctly folded proteins (Novotny et al., 1984). Thus, the analysis presented in this paper can be understood as the first steps toward a more complete elucidation of the details of protein:lipid interactions from a microscopic level. Two important findings that have bearing on structure prediction should be emphasized. First, proline residues act to break up the $\alpha$-helical structure and should be considered as possible hinge points for generation of conformational searches in tertiary structure. Second, the presence of aromatics at the interfaces should be viewed as a favorable partitioning state. This suggests that positioning of $\alpha$-helical segments in order to optimize the position of aromatics relative to the interface could be used in the construction of starting points for tertiary structure.

The computer resources of the Biomedical Engineering Department at Johns Hopkins were essential for this publication. Helpful comments on the presentation and text were contributed by Alan Grossfield. Additional helpful comments were provided by referees (from another journal) for the first submission of this manuscript in May, 1996.

Financial support from the Bard Foundation and the Department of Physiology is gratefully acknowledged.

## REFERENCES

Adams, P. D., I. T. Arkin, D. M. Engelman, and A. T. Brunger. 1995. Computational searching and mutagenesis suggest a structure for the pentameric transmembrane domain of phospholamban *Nat. Struct. Biol.* 2:154–162.

Baldwin, J. M. 1993. The probable arrangement of the helices in G protein-coupled receptors. *EMBO J.* 12:1693–1703.

Bassolino-Klimas, D., H. E. Alper, and T. R. Stouch. 1993. Solute diffusion in lipid bilayer membranes: an atomic level study by molecular dynamics simulation. *Biochemistry.* 32:12624–12637.

Breed, J., I. D. Kerr, R. Sankararamakrishnan, and M. S. P. Sansom. 1995. Packing interactions of Aib-containing helices: molecular modeling of parallel dimers of simple hydrophobic helices and of alamethicin. *Biopolymers.* 35:639–655.

Brooks, C. L. III, M. Karplus, and B. M. Pettitt. 1988. Proteins: A theoretical perspective of dynamics, structure, and thermodynamics. *In* Advances in Chemical Physics LXXI, John Wiley and Sons, New York.

Cherry, R. J., U. Muller, R. Henderson, and M. P. Heyn. 1978. Temperature-dependent aggregation of bacteriorhodopsin in dipalmitoyl and dimyristoyl phosphatidylcholine vesicles. *J. Mol. Biol.* 121:283–298, 1978.

Chiu, S.-W., M. Clark, V. Balaji, S. Subramaniam, H. L. Scott, and E. Jakobsson. 1995. Incorporation of surface tension into molecular dynamics simulation of an interface: a fluid phase lipid bilayer membrane. *Biophys. J.* 69:1230–1245.

Cramer, W. A., D. M. Engelman, G. V. Heijne, and D. C. Rees. 1992. Forces involved in the assembly and stabilization of membrane proteins. *FASEB J.* 6:3397–3402.

Creighton, T. E. 1993. Proteins: Structure and Molecular Properties, 2nd ed. W. H. Freeman, New York.

Cronet, P., C. Sander, and G. Vriend. 1993. Modeling of transmembrane seven helix bundles. *Protein Eng.* 6:59–64.

Damodaran, K. V., K. M. Merz, and B. P. Bager. 1995. Interaction of small peptides with lipid bilayers. *Biophys. J.* 69:1299–1308.

Deber, C. M., M. Glibowicka, and G. A. Woolley. 1990b. Conformations of proline residues in membrane environments. *Biopolymers.* 29: 149–157.

Deber, C. M., B. J. Sorrell, and G-Y. Xu. 1990a. Conformation of proline residues in bacteriorhodopsin. *Biochem. Biophys. Res. Commun.* 172: 862–869.

Do, H., D. Falcone, J. Lin, D. W. Andrews, and A. E. Johnson. 1996. The cotranslational integration of membrane proteins into the phospholipid bilayer is a multistep process. *Cell.* 85:369–378.

Edholm, O., O. Berger, and F. Jahnig. 1995. Structure and fluctuations of bacteriorhodopsin in the purple membrane: a molecular dynamics study. *J. Mol. Biol.* 250:94–111.

Engelman, D. M., T. A. Steitz, and A. Goldman. 1986. Identifying nonpolar transbilayer helices in amino acid sequences of membrane proteins. *Annu. Rev. Biophys. Biophys. Chem.* 15:321–353.

Feller, S. E., and R. W. Pastor. 1996. On simulating lipid bilayers with an applied surface tension: periodic boundary conditions and undulations. *Biophys. J.* 71:1350–1355.

Feller, S. E., Y. Zhang, and R. W. Pastor. 1995. Computer simulation of liquid/liquid interfaces. II. Surface tension-area dependence of a bilayer and monolayer. *J. Chem. Phys.* 103:10267–10276.

Furois-Corbin, S., J. C. Smith, and G. R. Kneller. 1993. Picosecond timescale rigid-helix and side-chain motions in deoxymyoglobin. *Proteins.* 16:141–154.

Gerstein, M., B. F. Anderson, G. E. Norris, E. N. Baker, A. M. Lesk, and C. Chothia. 1993. Domain closure in lactoferrin: two hinges produce a see-saw motion between alternative close-packed interfaces. *J. Mol. Biol.* 234:357–372.

Gray, T. M. N., and B. W. Matthews. 1984. Intrahelical hydrogen bonding of serine, threonine, and cysteine residues within $\alpha$-helices and its relevance to membrane-bound proteins. *J. Mol. Biol.* 175:75–81.

Grigorieff, N., T. A. Ceska, K. H. Downing, J. M. Baldwin, and R. Henderson. 1996. Electron-crystallographic refinement of the structure of bacteriorhodopsin. *J. Mol. Biol.* 259:393–421.

Hardy, B. J., and R. W. Pastor. 1994. Conformational sampling of hydrocarbon and lipid chains in an orienting potential. *J. Comp. Chem.* 15:208–226.

Hartsough, D. S., and K. M. Merz. 1993. Protein dynamics and solvation in aqueous and nonaqueous environments. *J. Am. Chem. Soc.* 115: 6529–6537.

Heijne, G. v. 1991. Proline kinks in transmembrane $\alpha$-helices. *J. Mol. Biol.* 218:499–503.

Heller, H., M. Schaefer, and K. Schulten. 1993. Molecular dynamics simulation of a bilayer of 200 lipids in the gel and in the liquid-crystal phases. *J. Phys. Chem.* 97:8343.

Henderson, R., J. M. Baldwin, T. A. Ceska, F. Zemlin, E. Beckmann, and K. H. Downing. 1990. Model for the structure of bacteriorhodopsin based on high-resolution electron cryomicroscopy. *J. Mol. Biol.* 213: 899–929.

Hermans, J., A. G. Anderson, and R. H. Yun. 1992. Differential helix propensity of small apolar side chains studied by molecular dynamics simulations. *Biochemistry.* 31:5646–5653.

Herzyk, P., and R. E. Hubbard. 1995. Automated method for modeling seven helix transmembrane receptors from experimental data. *Biophys. J.* 69:2419–2442.

Hirst, J. D., and C. L. Brooks III. 1995. Molecular dynamics simulations of isolated helices of myoglobin. *Biochemistry.* 34:7614–7621.

Holland, D. R., D. E. Tronrud, H. W. Plye, K. M. Flaherty, W. Stark, J. N. Jansonius, D. B. McKay, and B. W. Matthews. 1992. Structural comparison suggests that thermolysin and related neutral proteases undergo hinge-bending motion during catalysis. *Biochemistry.* 31:11310–11316.

Humphrey, W., I. Logunov, K. Schulten, and M. Sheves. 1994. Molecular dynamics study of bacteriorhodopsin and artificial pigments. *Biochemistry.* 33:3668–3678.

Jahnig, F. 1996. What is the surface tension of a lipid bilayer membrane? *Biophys. J.* 71:1348–1349.

Jahnig, F., and O. Edholm. 1992. Modeling of the structure of bacteriorhodopsin: a molecular dynamics study. *J. Mol. Biol.* 226: 837–850.

Kahn, T. W., and D. M. Engelman. 1992. Bacteriorhodopsin can be refolded from two independently stable transmembrane helices and the complementary five-helix fragment. *Biochemistry.* 31:6144–6151.

Kahn, T. W., J. M. Sturtevant, and D. M. Engelman. 1992. Thermodynamic measurements of the contributions of helix-connecting loops and of retinal to the stability of bacteriorhodopsin. *Biochemistry.* 31: 8829–8839.

Kovacs, H., A. E. Mark, J. Johansson, and W. F. v. Gunsteren. 1995. The effect of environment on the stability of an integral membrane helix: molecular dynamics simulations of surfactant protein C in chloroform, methanol, and water. *J. Mol. Biol.* 247:808–822.

Logunov, I., W. Humphrey, K. Shulten, and M. Sheves. 1995. Molecular dynamics study of the 13-*cis* form (bR548) of bacteriorhodopsin and its photocycle. *Biophys. J.* 68:1270–1282.

Loncharich, R. J., B. R. Brooks, and R. W. Pastor. 1992. Langevin dynamics of peptides: the frictional dependence of isomerization rates of *N*-acetylalanyl-*N'*-methylamide. *Biopolymers.* 32:523–535.

Lozier, R. H., R. A. Bogomolni, and W. Stoeckenius. 1975. Bacteriorhodopsin: a light-driven proton pump in *Halobacterium halobium. Biophys. J.* 15:955–967.

McPhalen, C. A., M. G. Vincent, D. Picot, J. N. Jansonius, A. M. Lesk, and C. Chothia. 1992. Domain closure in mitochondrial aspartate aminotransferase. *J. Mol. Biol.* 227:197–213.

Merz, K. M., Jr., and B. Roux. 1996. Biological Membranes: A Molecular Perspective from Computation and Experiment. Birkhauser Press, Boston.

Mogi, T., L. J. Stern, B. H. Chao, and H. G. Khorana. 1989. Structure-function studies on bacteriorhodopsin VIII. Substitutions of the membrane-embedded prolines 50, 91, and 186: the effects are determined by the substituting amino acids. *J. Biol. Chem.* 264:14192–14196.

Nagle, J. R. 1993. Area/lipid of bilayers from nmr. *Biophys. J.* 64: 1476–1481.

Novotny, J., R. Bruccoleri, and M. Karplus. 1984. An analysis of incorrectly folded protein models: implications for structure prediction. *J. Mol. Biol.* 177:787–818.

O'Neil, K. T., and W. F. DeGrado. 1990. A thermodynamic scale for the helix-forming tendencies of the commonly occurring amino acids. *Science.* 250:646–651.

Pastor, R. W. 1994. Molecular dynamics and Monte Carlo simulations of lipid bilayers. *Curr. Opin. Struct. Biol.* 4:486–492.

Paulsen, M. D., and R. L. Ornstein. 1995. Dramatic differences in the motions of the mouth of open and closed cytochrome P450BM-3 by molecular dynamics simulations. *Proteins.* 21:237–243.

Popot, J.-L., and D. M. Engelman. 1990. Membrane protein folding and oligomerization: the two-stage model. *Biochemistry.* 29:4031–4037.

Rapoport, T. A., M. M. Rolls, and B. Jungnickel. 1996. Approaching the mechanism of protein transport across the ER membrane. *Curr. Opin. Cell Biol.* 8:499–504.

Rees, D. C., L. DeAntonio, and D. Eisenberg. 1989. Hydrophobic organization of membrane proteins. *Science.* 245:510–513.

Roux, B. 1996. Commentary: surface tension of biomembranes. *Biophys. J.* 71:1346–1347.

Roux, B., and T. B. Woolf. 1996. Molecular dynamics of Pf1 coat protein in a phospholipid bilayer. *In* Biological Membranes: A Molecular Perspective from Computation and Experiment. K. M. Merz, Jr., and B. Roux, editors. Birkhauser Press, Boston. 555–587.

Sankararamakrishnan, R., and M. S. P. Sansom. 1994. Kinked structures of isolated nicotinic receptor M2 helices: a molecular dynamics study. *Biopolymers.* 34:1647–1657.

Sankararamakrishnan, R., N. Sreerama, and S. Vishveshwara. 1991. Characterization of proline-containing right-handed α-helix by molecular dynamics studies. *Biophys. Chem.* 40:97–108.

Sankararamakrishnan, R., and S. Vishveshwara. 1990. Conformational studies on peptides with proline in the right-handed α-helical region. *Biopolymers.* 30:287–298.

Sankararamakrishnan, R., and S. Vishveshwara. 1992. Geometry of proline-containing α-helices in proteins. *Int. J. Pept. Res.* 39:356–363.

Sankararamakrishnan, R., and S. Vishveshwara. 1993. Characterization of proline-containing α-helix (helix F model of bacteriorhodopsin) by molecular dynamics studies. *Proteins.* 15:26–41.

Sansom, M. S. P. 1992. Proline residues in transmembrane helices of channel and transport proteins: a molecular modeling study. *Prot. Eng.* 5:53–60.

Sansom, M. S. P., H. S. Son, R. Sankararamakrishnan, I. D. Kerr, and J. Breed. 1995. Seven-helix bundles: molecular modeling via restrained molecular dynamics. *Biophys. J.* 68:1295–1310.

Schlenkrich, M., J. Brickmann, A. D. MacKerell, Jr., and M. Karplus. 1996. An empirical potential energy function for phospholipids: criteria for parameter optimization and applications. *In* Biological Membranes: A Molecular Perspective from Computation and Experiment. K. M. Merz, Jr., and B. Roux, editors. Birkhauser Press, Boston.

Sharff, A. J., L. E. Rodseth, J. C. Spurlino, and F. A. Quicho. 1992. Crystallographic evidence of a large ligand-induced hinge-twist motion between the two domains of the maltodextrin binding protein involved in active transport and chemotaxis. *Biochemistry.* 31:10657–10663.

Shen, L., D. Bassolino, and T. Stouch. 1996. Structure and interaction of a transmembrane polyalanine α-helix with a DMPC bilayer studied by multi-nanosecond molecular dynamics simulation. *Biophys J.* 70:375*a*. (Abstr.).

Soman, K. V., A. Karimi, and D. A. Case. 1991. Unfolding of an α-helix in water *Biopolymers.* 31:1351–1361.

Subramaniam, S., M. Gerstein, D. Oesterhelt, and R. Henderson. 1993. Electron diffraction analysis of structural changes in the photocycle of bacteriorhodopsin. *EMBO J.* 12:1–8.

Suwa, M., T. Hirokawa, and S. Mitaku. 1995. A continuum theory for the prediction of lateral and rotational positioning of α-helices in membrane proteins: bacteriorhodopsin. *Proteins.* 22:363–377.

Taylor, W. R., D. T. Jones, and N. M. Green. 1994. A method for α-helical integral membrane protein fold prediction. *Proteins.* 18:281–294.

Treutlein, H. R., M. A. Lemmon, D. M. Engelman, and A. T. Brunger. 1992. The glycophorin A transmembrane domain dimer: sequence-specific propensity for a right-handed supercoil of helices. *Biochemistry.* 31:12726–12732.

Tu, K., D. J. Tobias, J. K. Blaise, and M. L. Klein. 1996. Molecular dynamics investigation of the structure of a fully hydrated gel phase DPPC bilayer. *Biophys. J.* 70:595–608.

Tu, K., D. J. Tobias, and M. L. Klein. 1995. Constant pressure and temperature molecular dynamics simulation of a fully hydrated liquid crystal phase dipalmitoylphosphatidylcholine bilayer. *Biophys. J.* 69: 2558–2562.

Tuffery, P., C. Etchebest, J.-L. Popot, and R. Lavery. 1994. Prediction of the positioning of the seven transmembrane α-helices of bacteriorhodopsin: a molecular simulation study. *J. Mol. Biol.* 236: 1105–1122.

Van Buren, A. R., and H. J. C. Berendsen. 1993. Molecular dynamics simulation of the stability of a 22-residue α-helix in water and 30% trifluoroethanol. *Biopolymers.* 33:1159–1166.

Venable, R. M., Y. Zhan, B. J. Hardy, and R. W. Pastor. 1993. Molecular dynamics simulations of a lipid bilayer and of hexadecane: an investigation of membrane fluidity. *Science.* 262:223–226.

Williams, K. A., and C. M. Deber. 1991. Proline residues in transmembrane helices: structural or dynamic role? *Biochemistry.* 30: 8919–8923.

Woolf, T. B. 1996. Molecular dynamics simulations of individual bacteriorhodopsin helices. *Biophys. J.* 70:377*a*. (Abstr.).

Woolf, T. B., and B. Roux. 1994. Molecular dynamics simulation of the gramicidin channel in a phospholipid bilayer *Proc. Natl. Acad. Sci. USA.* 91:11631–11635.

Woolf, T. B., and B. Roux. 1996. Structure, energetics, and dynamics of lipid-protein interactions: a molecular dynamics study of the gramicidin A channel in a DMPC bilayer. *Proteins.* 24:92–114.

Xu, D., M. Sheves, and K. Schulten. 1995. Molecular dynamics study of the M412 intermediate of bacteriorhodopsin. *Biophys. J.* 69: 2745–2760.

Xu, D., C. Martin, and K. Schulten. 1996. Molecular dynamics study of early picosecond events in the bacteriorhodopsin photocycle: dielectric response, vibrational cooling, and the J, K intermediates. *Biophys. J.* 70:453–460.

Yun, R. H., A. Anderson, and J. Hermans. 1991. Proline in α-helix: stability and conformation studied by dynamics simulation. *Proteins.* 10:219–228.

Zhang, Y. S., S. E. Feller, B. R. Brooks, and R. W. Pastor. 1995. Computer simulation of liquid/liquid interfaces. I. Theory and application to octane/water. *J. Chem. Phys.* 103:10252–10266.

Zhou, F., A. Windemuth, and K. Schulten. 1993. Molecular dynamics study of the proton pump cycle of bacteriorhodopsin. *Biochemistry.* 32:2291–2306.